UDC 539.4

The Wear of Dies for Mechanical Clinching when Joining of Advanced High-Strength Steel Sheets*

L. Kaščák,[a,1] J. Mucha,[b,2] E. Spišák,[a,3] and R. Kubík[a,4]

[a] Technical University of Košice, Košice, Slovakia

[b] Rzeszów University of Technology, Rzeszów, Poland

[1] lubos.kascak@tuke.sk

[2] j_mucha@prz.edu.pl

[3] emil.spisak@tuke.sk

[4] rene.kubik@tuke.sk

УДК 539.4

Износ штампа механического пресса в процессе клинч-соединения листов из высокопрочных сталей методом холодной формовки

Л. Кащак[а], Я. Муха[б], Э. Спишак[а], Р. Кубик[а]

[а] Технический университет в Кошице, Кошице, Словакия

[б] Технологический университет Жешува, Жешув, Польша

Исследуется износ рабочей части механического пресса при клинч-соединении листов из легированной высокопрочной стали H220PD+Z с гальваническим покрытием методом холодной формовки (пуклевка). Точечное соединение листов осуществляется с помощью жесткого штампа и пуансона круглого сечения малого диаметра (без движущихся частей) из инструментальной стали с нанесенными PVD покрытиями трех типов: ZrN, CrN и TiCN MP. Износ рабочей части штампа с соответствующим покрытием оценивается после проведения 300 операций пуклевки. Сравнение полученных экспериментальных данных с результатами конечно-элементного расчета показывает их удовлетворительное соответствие и подтверждает, что износ рабочей части штампа происходит в основном вблизи круговой границы штампа и пуансона.

Ключевые слова: клинч-соединение, износ, штамп, PVD покрытие, метод конечных элементов.

Introduction. The need for joining of dissimilar, hard-to-weld or lightweight materials has evolved into the development of rapid and mechanical joining methods such as clinching, clinch-riveting, or self-piercing riveting [1]. Mechanically clinched joints are produced by controlled, severe plastic deformation of two or more parts in the form of sheet-metal. These materials are formed by the movement of punch into die [2]. Severe plastic deformation of joined materials takes place locally, resulting in the generation of an interlock between the sheets [3]. While the punch geometry is relatively simple, cavities of the dies are often complex-shaped surfaces with geometry specially designed to make

* Paper presented at the International Scientific Conference on Progressive Technologies and Materials in Mechanical Engineering (PRO-TECH-MA 2017), June 20–23, 2017, Bardejov Spa (Slovakia).

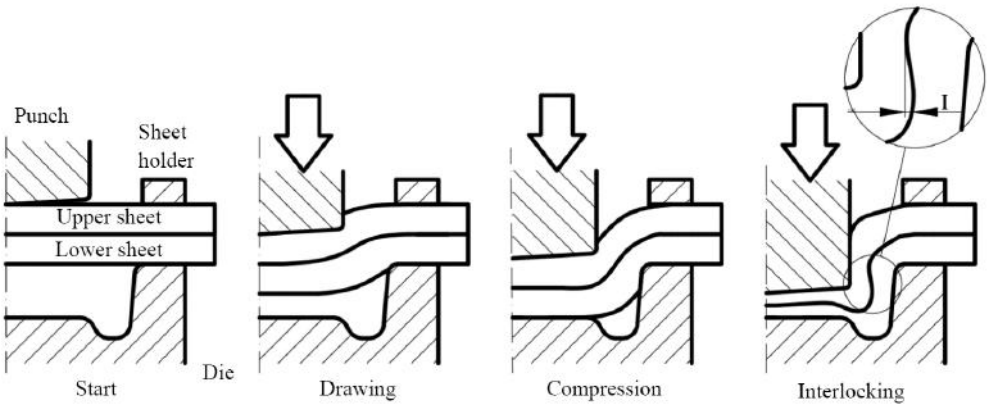

Fig. 1. Particular steps of round clinching with rigid die [5].

possible the interlocking of joined sheets. Dies for mechanical clinching can be rigid or extensible [4]. Extensible dies consist of sliding, sometimes referred as flexible elements that make possible flowing of joined materials in the radial direction. Radial flow of the sheet materials also takes place in the rigid dies, but only within the specially formed die cavity. The joint forming process occurs in three steps, which are referred to as: drawing, compression, and interlocking [5]. The principle of the round mechanical clinching with a rigid die is shown in Fig. 1. The punch is used to draw two or more sheets downwards, directly into the cavity of the rigid die, which step is known as the drawing step of joint forming process. Prior to it, both sheets are fixed by the holder to prevent their undesirable movement outside of the joining/forming area. The drawing step is terminated when the lower sheet material reaches the anvil of the die.The downward progression of the punch causes a compressive impact on both sheet materials. The thickness of both materials is being reduced in this step, which is known as the compression. As the materials reduce their thickness, they are also forced to flow radially – towards the groove of the die, which is also shaped to make possible the interlocking process. The interlocking process results in the specific "S" shape of the neck area of mechanically clinched joint. The interlocking parameter is also shown in detail in Fig. 1 (designated as "I"). This process is also referred to as the one-step mechanical joining. The mechanically clinched joints can be produced with more steps as well. A typical instance of two-step clinching is the so-called "flat "clinching. This joining method was developed to overcome problems related to the joint's protrusion that is present in the conventionally clinched joints. Typical round clinched joint is produced in the first step. The external protrusion is subsequently flattened to the plane of sheet [6]. However, flat clinched joints could be produced using one-step clinching when specially formed dies are utilized. In that case, material flow of joined materials takes place in the opposite direction to the punch movement [7]. The mechanical clinching joining methods are very similar, they can either be part of one- or two-step groups, hence systematic classification is hard to develop. Besides, there is a constant development of new concepts and refinement of the existing ones in the area of mechanical clinching. New processes, which do not fall into older classifications, are being permanently developed. One of those processes is a hybrid resistance spot clinching process, which has been designated as a resistance spot clinching technique. It combines the resistance spot welding with the mechanical clinching. During the downward movement of punch a low-level short-term electrical current passes through both joined sheets when the forming force reaches about a half of its total value. The punch retracts to its initial position when the specific level of forming force is reached [8].

Joining of advanced high-strength steel (USS) sheets or ultra-high-strength (UHS) ones requires some special treatment. The UHS steels are of special interest because they are replacing mild steel sheets to reduce the weight of automobile and improve the safety of driver and passengers. The tensile strength of this type of materials exceeds 1 GPa [9]. Joining of such materials by the mechanical clinching is quite problematic, because of their low ductility. Despite this, new methods have been proposed to join UHS and AHS steel sheets. These methods include the optimization of die cavity shape, adding a flexible element into the die cavity, or use punches with very high compressive strength [10–12]. Joining of such materials leads to the increased wear of the clinching tool caused by different hardening process of steel sheets during their cold forming. Hence the lifetime of the tools correlates with the material type to be joined [13]. When joining UHS or AHS steel sheets, the tools from the appropriate materials subjected to heat or/and surface treatment are utilized [14]. One of the possibilities to reduce the forming tool wear is the application of PVD coating [15]. Despite excessive amount of publications on the mechanical clinching of UHS or AHS steel, there is a lack of information describing the tool life or wear mechanisms occurring during joining of these types of materials. The research results regarding the tool life when clinching the alloy quality low-carbon steel sheets with the thickness of 1.0 mm and ultimate strength of 420 MPa were published in [16], where insufficient tool life was observed. The latter corresponded to the production of about 5,000 mechanically clinched joints, and tool's failure occurred due to its tip breakage. However, the number of joints produced using one pair of tools (punch and die) declared by the manufacturer should be much higher, namely about 100,000 mechanically clinched joints. As previously stated, this value strongly depends on the type of joined material [17].

This study is focused on the surface variations of the die cavity and surrounding areas during the mechanical clinching of the AHS steel sheets. The PVD coatings (CrN, ZrN, and TiCN) were deposited on the clinching tools to improve the tool wear resistance. Because of joining of high-strength steel sheets, wear mechanisms' occurrence is expected even in the early period of the tool life, which was set to 300 produced joints per each PVD coating. The experimental results were compared to the results of finite element analysis (FEA), which was carried out via the static implicit approach. The behavior of the die in the calculation process was set to deformable one. This approach makes possible to evaluate the stress and strain levels, as well as their localization at the surface of the die. Both types of results are analyzed and discussed.

1. **Experimental Procedure**. The hot-dip galvanized steel sheets were joined by utilizing the one step, round clinching with a rigid die. This process doesn't require any additional fasteners – both steel sheets are joined by the action of severe plastic deformation [18]. The die is the main element influencing the interlock formation process. Its geometry determines the materials flow when both joined materials are drawn into its cavity. The active parts of the clinching tool are the punch (Fig. 2a) and the die (Fig. 2b). Geometry and dimensions of both active parts are shown in the Fig. 2c. The curved surface of die cavity was classified into five areas (Fig. 2d): *OD* – the surrounding of the die cavity, *VD* – the top surface of the die cavity, *ROD* – the radius of the surrounding of the die cavity, *OVD* – the surrounding of the protrusion in die cavity, and *RVD* – the radius between areas of *VD* and *RVD*. The punch and the die were manufactured from the steel of grade 1.3343, which is classified as a high-speed steel (also known as HSS, M2 grade steel). This material is mainly utilized for cutting tools as well as for cold working tools in consideration of its very high toughness.

Chemical composition of 1.3343 tool steel was analyzed by the portable hybrid spectrometer Belec Compact Port as follows: 0.92% C, 0.31% Si, 0.33% Mn, 0.019% P, 0.005% S, 3.88% Cr, 4.76% Mo, 1.85% V, and 6.36% W. Both tools (punch and die) were processed by heat treatment, i.e., hardened up to 55–56 HRC. The tools were processed by

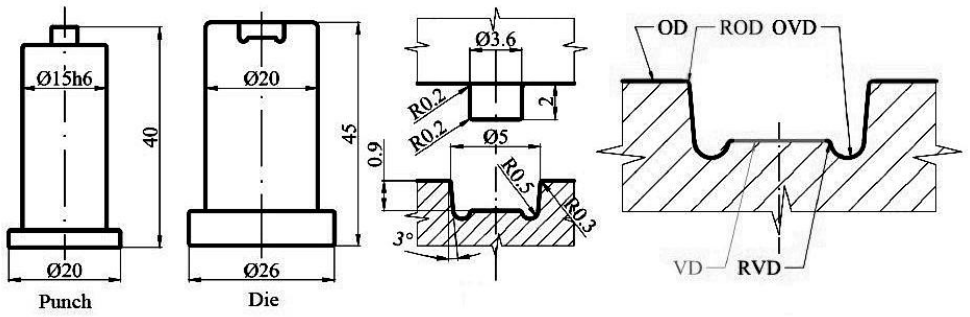

Fig. 2. Geometry of punch and die (a, b, c) and areas of the die cavity (d).

the grinding machine to the final roughness of $Ra = 0.2$ μm before the coating deposition process. Three types of PVD coatings such as CrN, ZrN, and TiCN MP were subsequently deposited on the surfaces of the punch and the die by LARC (Lateral Rotating Arc Cathode) process. The chemical composition of individual coatings was determined by GD-OES method (Glow Discharge Optical Emission Spectroscopy). GD-OES tests were carried out on the test samples made together with the tools. Results of the GD-OES tests showed deep level concentration profiles of the elements Zr, Ti, Al, N, and C and changes of their concentration across the depth of 5 μm. A certain amount of titanium was present at the interface of the substrate material and coating, being a part of the intermediate surface layer that increased the coating–substrate adhesion.

The thickness of coatings was another measured parameter assessed by the Calotest method. The thickness values of the individual coating are shown in Table 1 along with the values of microindentation hardness and indentation modulus of all mentioned PVD coatings.

T a b l e 1

Basic Properties of PVD Coatings

Coating	Substrate material	Hardness of substrate (HRC)	Indentation modulus (GPa)	Thickness (μm)	Indentation hardness (GPa)
ZrN	1.3343 steel	55–56	407	2.96	29
TiCN MP			485	3.35	51
CrN			325	2.04	27

The values of indentation modulus and indentation hardness were obtained through microindentation tester (TTX-NHT S/N) with Berkovich diamond indenter. The maximum load of 60 mN was applied to indenter, which worked in the sinusoidal mode with an amplitude of 6 mN and frequency 15 Hz. Hold time was 10 s. Measured values of indentation hardness are shown in Table 2. The surface microgeometry parameters of the individual surface of the coating according to ISO 4287 (Profilometer SJ-201) and ISO 25 178 (Confocal microscope – magn 20x) were determined as well. The parameters according to ISO 4287 were measured in longitudinal (in the direction of grinding) and transverse (perpendicularly to the direction of grinding) direction, as shown in Table 2.

Table 2

Surface Microgeometry Parameters of PVD Coatings

Coating	Parameters according to ISO 4287 (μm)					
	Ra_{long}	Rz_{long}	Rq_{long}	Ra_{trans}	Rz_{trans}	Rq_{trans}
ZrN	0.22	1.96	0.29	0.17	1.35	0.22
TiCN	0.31	2.42	0.39	0.33	3.31	0.45
CrN	0.22	5.55	0.32	0.30	2.83	0.40
	Parameters according to ISO 25178 (μm)					
	Sa	*Sq*	*Sp*	*Sv*	*Sz*	*Sa*
ZrN	0.35	0.47	3.89	8.86	12.75	0.37
TiCN	0.37	0.51	7.04	2.27	9.31	0.38
CrN	0.20	0.28	3.15	1.42	4.58	0.22

The surface of all coatings was observed by scanning electron microscopy (JEOL JSM-7000F) and Vega3 Tescan to obtain information about surface topography of ZrN, TiCN MP and CrN coatings. EDX qualitative microanalysis could also be performed along with the acquisition of SEM images. The surface topography of ZrN, TiCN MP and CrN coatings scanned on the testing sample surfaces (substrate 1.3343 steel, 55–56 HRC) are shown in Fig. 3. Some particles in the form of spheres were observed in the case of all three coatings. EDX analysis confirmed the presence of zirconium, titanium, and chromium for appropriate coatings. These particles occurred on the surface of each coating because of the deposition process used (cathodic arc sputtering).

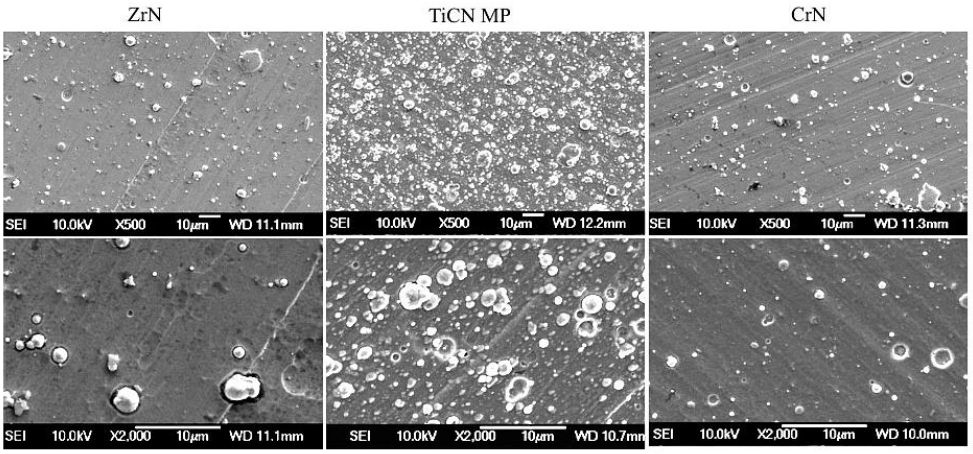

Fig. 3. Surface topography of ZrN, TiCN MP, and CrN coating on testing samples.

The hot-dip galvanized high-strength low alloy (HSLA) steels, sometimes referred as microalloyed steels, are produced to provide better mechanical properties and better corrosion resistance in the atmospheric conditions [19]. H220PD+Z steel sheets with a thickness of 0.8 mm were joined by clinching with the rigid die. This type of steel is microalloyed with Ti and Nb; its carbon content does not exceed 0.08%. The chemical

composition of the joined material was determined by the optical emission spectroscopy (OES) method. The results of determination of the chemical composition of H220PD+Z steel by the OES method are shown in Table 3. The steel sheets were hot-dip galvanized with the thickness of zinc layer of 10 μm on both sides of the sheet. Zinc quantity for H220PD+Z steel is 100 g/m^2 for the Z100MBO grade. The microstructure of H220PD+Z steel consists of ferrite and cementite. The mechanical properties of H220PD+Z steel sheets were determined by the standardized tensile tests carried out according to STN EN ISO 6892-1 standard. These properties were measured in three directions (0, 45, and 90°). The results of the tensile test (Table 4) of joined materials were used for the definition of material behavior during its deformation in FEA simulation of the mechanical joining.

T a b l e 3

Chemical Composition of H220PD+Z steel (wt.%)

C	Mn	Si	P	S	Al	Cu
0.004	0.415	0.10	0.042	0.004	0.035	0.011
Ni	Cr	Ti	V	Nb	Mo	
0.017	0.031	0.037	0.002	0.026	0.005	

T a b l e 4

Mechanical Properties of H220PD+Z Steel Sheets

Direction (deg)	$R_{p0.2}$, MPa	R_m, MPa	A_{80}, %	A_g, %	r	n
0	219	385	34.5	21.8	1.172	0.235
45	225	368	37.5	25.3	1.782	0.231
90	238	382	35.8	22.3	1.823	0.290

2. **Simulation Procedure**. Most mechanical clinching joining processes are simulated under 2D axisymmetric conditions. Such conditions make possible to simplify and speed up the computation process. Furthermore, tools do not need to be modeled as whole bodies; they can be simplified as well. Joined materials in the form of sheets are modeled as deformable bodies and (most of the time) tools are considered as rigid bodies undergoing only small elastic deformations, which are negligible. However, when assessing stress and strain levels in tools during the joining process, the bodies should be modeled as deformable ones. Here, a static implicit approach in the 2D axisymmetric formulation was utilized to simulate the round clinching joining process (with a rigid die) of two steel (H220PD+Z) sheets. Punch and die shown in the Fig. 2 were simplified according to the 2D simulation requirements. Geometrical model and boundary conditions as the partial input for the finite element analysis are shown in Fig. 4a.

Parts of the tools and both sheet materials, as shown in Fig. 4a, are split into two regions: (i) with a fine mesh and (ii) with a coarse mesh. Contact areas or areas undergoing large deformations must be meshed with smaller elements than the rest of the model. It is clear from Fig. 4b that the simulation results are stable when 0.2-mm sized elements are used. However, this specific case should be meshed with elements of 0.1 mm at least, due to the high curvature of the die cavity. 0.2-mm sized elements poorly describe the complex geometry of die and lead to poor convergence behavior of the solving process. Therefore, 2D axisymmetric plane elements were used for meshing.

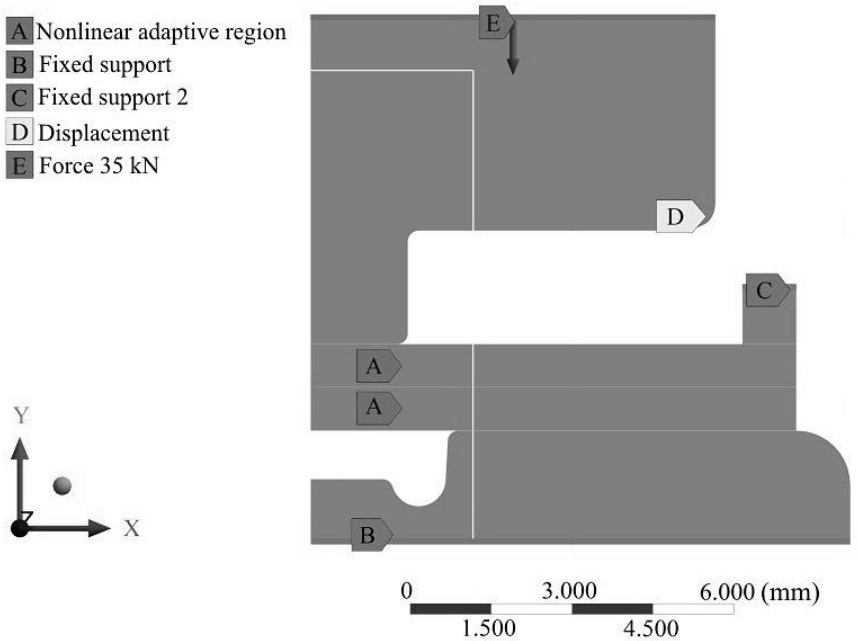

a

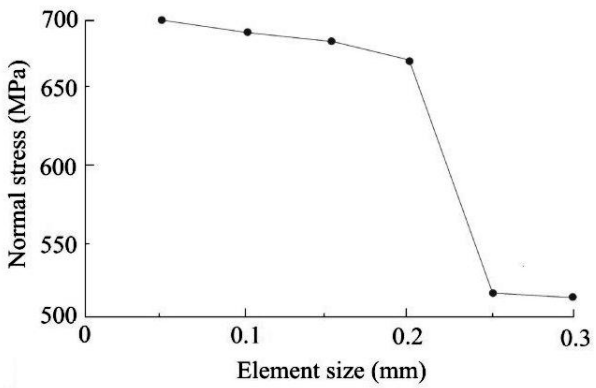

b

Fig. 4. Geometrical model, boundary conditions (a) and mesh sensitivity analysis (b).

These elements are known as PLANE182 low-order elements in ANSYS with two translational degrees of freedom in *X* and *Y* directions. Both joined materials in the form of sheets are provided with the nonlinear adaptive region boundary condition, which makes it possible to rectify the excessively distorted elements. This is a common problem related to mechanical joining or forming of materials in general. Both sheets undergo large deformations during the joint forming process, and their thickness is significantly reduced. Due to this, the mesh quality criterion was utilized to make possible to "repair" the distorted mesh elements by applying an angle-based criterion, which initiated the mesh repairing process. Besides meshing, two isotropic material hardening models (bilinear and multilinear one) were adapted for all deformable bodies in the model. These models are associated with the von Misses plasticity model, which is suitable for simulating the plasticity of high-strength materials under isotropic conditions [20]. The summarized values of individual material models used for FEA are listed in Table 5.

T a b l e 5

Material Models for FEA of Clinching Joining

Material model	Steel	$R_{p0.2}$, MPa	E, GPa	ν	E_T, MPa
Bilinear	1.3343	2000	210	0.3	1000
Multilinear	H220PD+Z	219			–

The parameters required for the material model of steel sheets were obtained by tensile testing of samples. Tests were carried out according to standard STN EN ISO 6892-1. Engineering stress-strain data were converted to true stress-strain representation, and the elastic portion was subtracted to get individual points of multilinear isotropic hardening model. The values required for defining the bilinear isotropic hardening were obtained from the manufacturer of the tool material (Böhler). Tools were modeled as a single body made of tool steel, while the presence of coating was disregarded.

3. **Results and Discussion**. In total, 300 mechanically clinched joints was produced by each pair of tools, i.e., punch and die covered with CrN, TiCN MP, or ZrN coating. The total amount of 900 joints were produced. The surface of the die cavity was scanned by SEM both at the initial state and after 300 joining cycles for each observed PVD coating. The SEM results were extended with the EDX analysis. FEA results should confirm the localization and orientation of the load maximum values during the individual joint forming phases of mechanical clinching of H220PD+Z steel sheets. The initial appearances of the die surface and the coating deposited on it are shown in Fig. 5a. The detailed view of the die cavity surface is shown in Fig. 5b. The first image of Fig. 5a shows the designation system of individual areas on the surface of die cavity when scanning perpendicularly to the surface. Individual "balloons" designate the circumferential area of the die cavity, not specific points. As to *VD* and *OD* areas, *VD* area represents the inner protrusion of the die cavity (circular area), and *OD* area represents the surrounding of the die cavity. Each SEM image has a designation in the right bottom corner describing the coating type scanned. The macro-level images of the die surface are shown in Fig. 5a, c, and e, while the detailed views on the surface of die cavity are shown in Fig. 5b, d, and f.

The surface of individual coatings (CrN, TiCN MP and ZrN) at the initial state exhibited no distinct forms of damage, wear or other forms of defect that could negatively influence the proper function of the tools for the mechanical clinching. Very small particles of spherical shape (approx. 2 μm in diameter), as shown in Fig. 3, were visible only when the surface was scanned with higher magnifications. As previously mentioned, these particles were analyzed by the EDX qualitative microanalysis, which confirmed the presence of zirconium (ZrN coating), titanium (TiCN MP coating), and chromium (CrN coating) in the spherical particles on the surface of corresponding coatings. Very distinctive milling marks were visible in the *OVD* area, already at the magnitude of 500x (in all three cases). Those areas were detected as potential areas of wear in the form of zinc particles entrapping in the groove of milling mark due to the material flow during the compression and interlocking phases of the joint forming process. However, the significance of this drawback was proven by the subsequent experimental findings. Surfaces of individual PVD coatings were after the production of 300 mechanically clinched joints by each coated pair of tools (punch and die).

Some forms of wear occurred after 300 mechanically clinched joints were produced by each pair of tools covered with CrN, TiCN MP, and ZrN coatings. Surfaces of individual dies covered with PVD coatings after the production of 300 mechanically clinched joints are shown in Fig. 6. The most disrupted area of the surface of die cavity was the *ROD* area (the radius of the surrounding die cavity), which is the very typical area for dies. The EDX

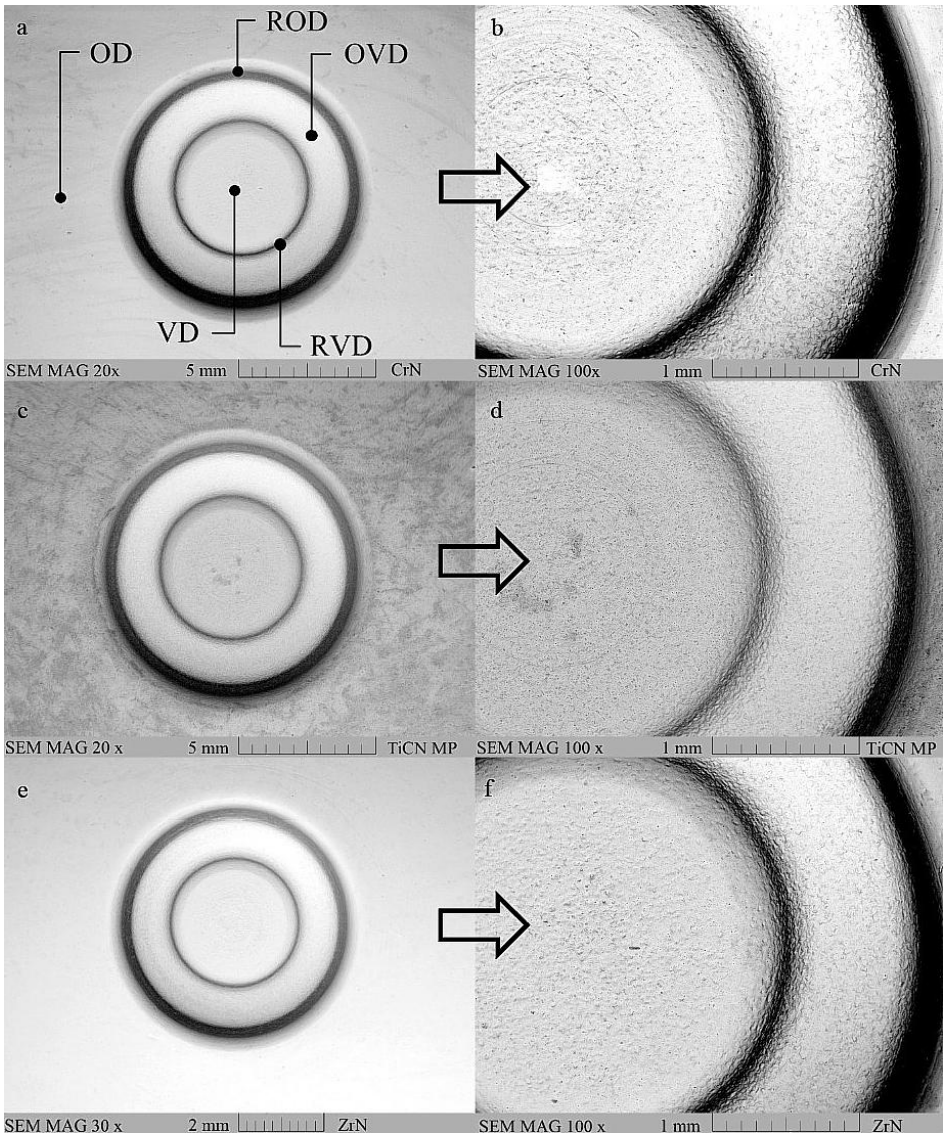

Fig. 5. The initial state of the surface of die cavity with deposited CrN, TiCN MP, and ZrN coatings (SEM).

qualitative analyses were carried out by scanning the die cavity surfaces, which provided a deeper insight into the elementary processes that take place during the joining of H220PD+Z steel sheets. The results of EDX analysis are depicted in Fig. 6a, c, and e in correspondence with the matching figures of individual coatings.

The macrolevel images of die cavity for each coating (CrN, TiCN MP, and ZrN) after 300 cycles of mechanical joining of H220PD+Z steel sheets are shown in Fig. 6a, c, and e. All three images show the area where the EDX analysis was performed. Figure 6b, d, and f show the *ROD* area after 300 cycles of mechanical joining of H220PD+Z steel sheets and exact location of EDX analysis. No wear or distinctive degradation of the coating was detected for die covered with the TiCN MP coating. A small amount of zinc and titanium was detected in the *ROD* area by the qualitative EDX microanalysis. Small spherical particles observed on the surface of testing samples (Fig. 3) were almost not visible at

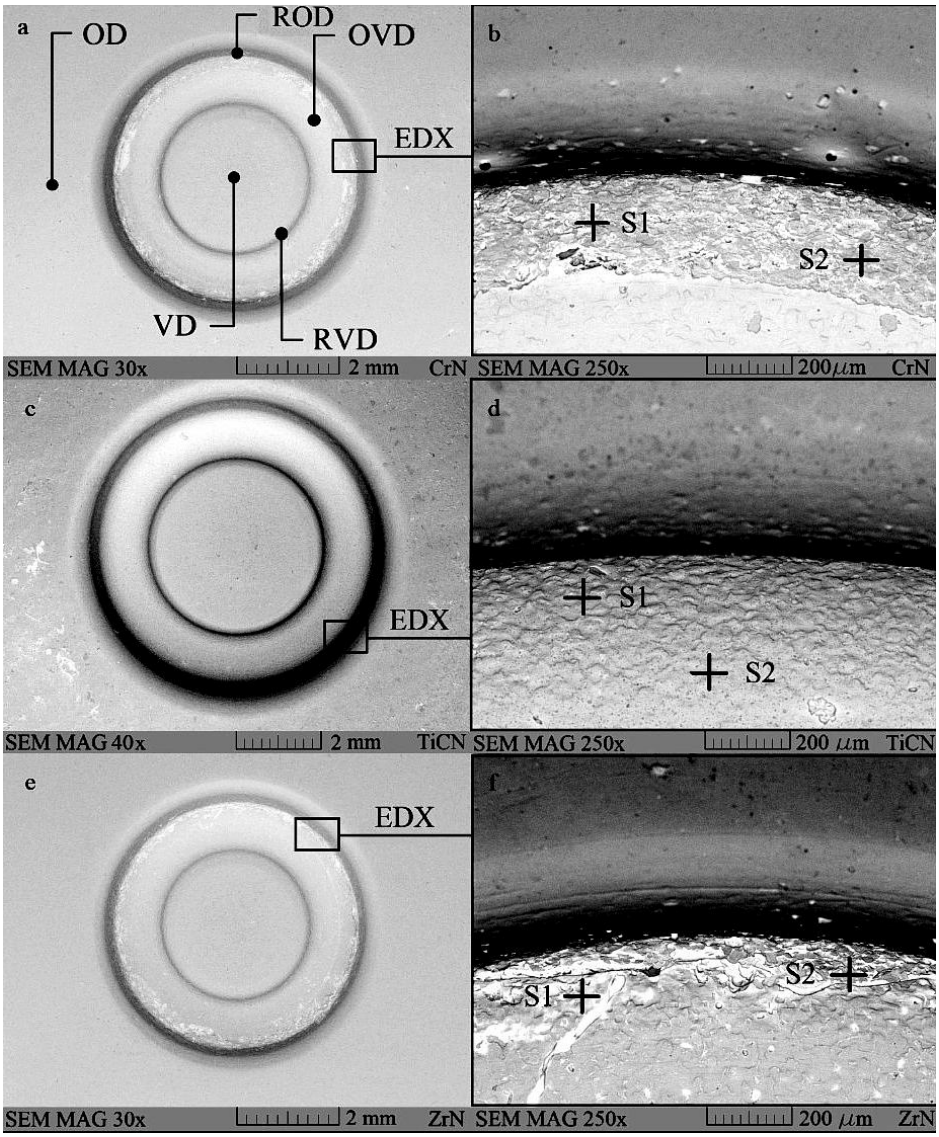

Fig. 6. State of the surface of the *ROD* area with deposited CrN, TiCN MP, and ZrN coatings (SEM) after 300 produced joints.

higher magnitudes (500x). Some of them were removed, especially in the areas of intensive material flow and friction (*OD* area, very close to the die cavity). However, surface integrity was observed in the case of TiCN MP coating. Some wear in the form of galling was observed in the case of dies covered with the CrN and ZrN coatings – Fig. 6b and f. Zinc and iron were detected in the *ROD* areas by the qualitative EDX analysis. Hence this type of wear was observed in the *ROD* area as well. A galling form of wear along with adhesion is typical for situations where surfaces slide upon each other, such as metal forming processes. Mechanical clinching can also be considered as metal forming operation. Galling could be observed in processes that have high load along with low speed and vice versa. About this process, there is a local galling of zinc from the protective coating of the sheet to the surface of the die in the *ROD* area, because materials with higher hardness (such as nitrides) are resistant to the galling. As a result of local galling, a certain amount of

zinc is being stuck (or even adhesively bonded) to the surface. Besides the *ROD* area (CrN and ZrN coating), there were only minor traces of material flow observed on the surface of the rest areas defined on the curved surface of the die cavity. The most frequent form of this was the removal of small spherical particles from the coating's surface at the areas of *VD* and *OD*. This phenomenon is shown in the Fig. 7, where the *VD* area of CrN coating is shown at the initial state (Fig. 7a) and after 300 mechanically clinched joints (Fig. 7b).

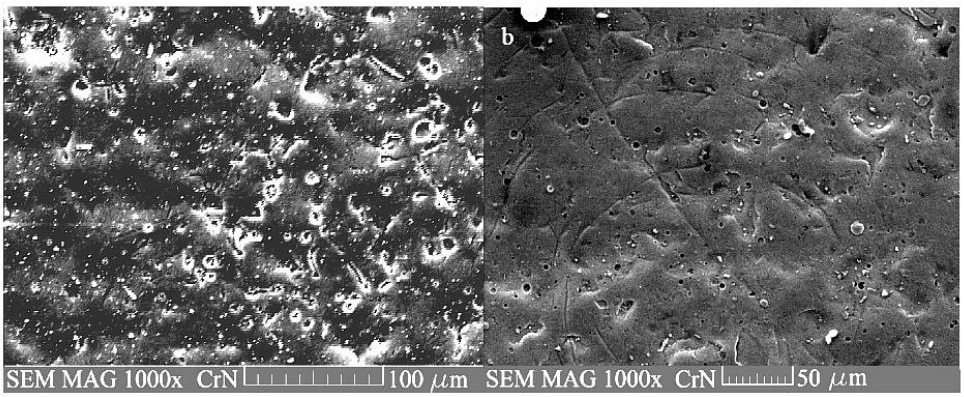

Fig. 7. State of the surface of the *VD* area with deposited CrN coating at the initial state (a) and after 300 joining cycles (b).

Galling and adhesion are typical for situations with the sliding of individual surfaces, especially when no lubricant is used. However, the main driving factor of galling is compressive forces that compress the surfaces towards each other. Because a certain amount of force is required to drive the punch downwards (along with the joined material), compressive forces or pressure occurs at the punch–upper sheet, upper–lower sheet and lower sheet–die interface. This phenomenon is also known as the contact pressure. Contact pressure is determined by the shape of the surfaces and magnitude of the normal force. Moreover, the contact pressure generates the stresses in the material, which is close to the contact. Finite element analyses were carried out to identify the level of contact pressure in the individual contact areas mentioned above. Presence of the coating on the die and punch was not included in the analyses. All bodies were modeled as flexible, individual parameters and their values representing the elasticity and plasticity are shown in Table 5. The static implicit approach was utilized. Results of the finite element analysis are shown in Fig. 8. Fig. 8a shows the evolution of normal stress (in the global *Y* direction) during the individual joint forming phases of mechanical clinching with rigid die whereas results are related to the contour of the die cavity. The material flow during individual joint forming phases of mechanical clinching with the rigid die is shown in Fig. 8b. The result shows the location of maximum contact pressure value. This is a restriction of ANSYS software, where the contact pressure cannot be displayed in any other manner because of the conflict between the results scoping and remeshing criterion applied. The contact pressure cannot be evaluated on the contour of the die because remeshing process changes the position of individual nodes of the mesh during the solution process and contact pressure evaluation requires those nodes for calculation of the contact pressure values.

The FEA results confirmed that *ROD* area of the die cavity is one of the most loaded parts of the die cavity contour during drawing and compression stages of the mechanical clinching. Given this, the RVD area can also be considered as the critical one. These areas undergo large compressive stresses in the drawing and compression stages of the joint forming process, which could be seen in Fig. 8a and 8c. Analysis of the contact pressure in the die/lower sheet interface showed that the *RVD* and the *ROD* areas are the locations of

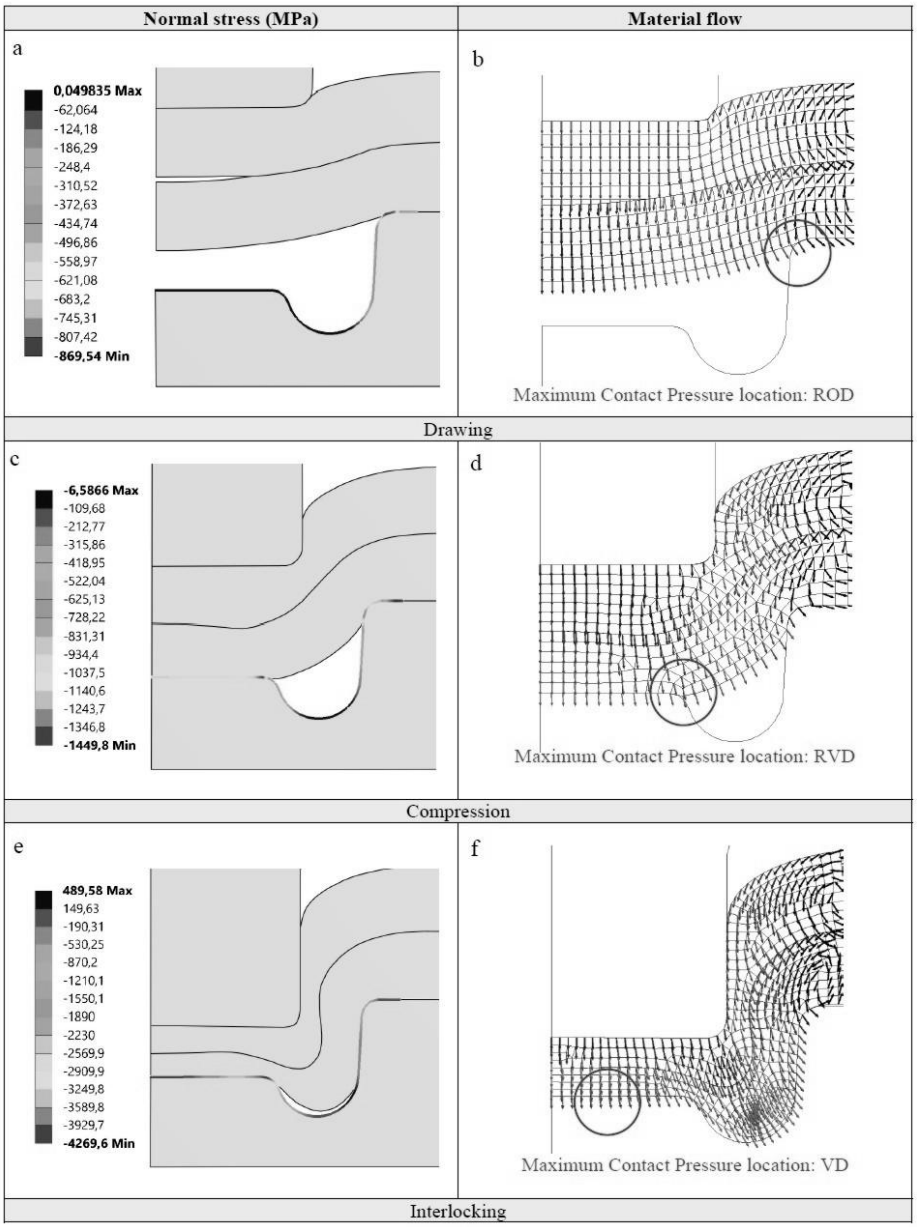

Fig. 8. Evolution of the normal pressure at the die cavity contour (a, c, e), material flow during the joining process via clinching (b, d, f).

the maximum contact pressure when steel sheets are drawn and compressed. Levels of the contact pressure and the normal stress reached sufficient level to initiate the galling and the adhesion wear mechanisms. The RVD area of the die cavity should wear by the same manner as the *RVD* area, based on the results of finite element analyses. However, there were no distinctive traces of wear in the *RVD* area as were detected in the *ROD* area of the die cavity covered with CrN and ZrN coatings. This situation changed when moving from compression to interlocking stage. Both maximum normal stress and contact pressure values move towards the center axis of the die cavity when transferring from the compression to the interlocking phase. This phenomenon is shown in Fig. 8e and 8f.

Maximum normal stress and contact pressure values are evaluated in the *VD* area of the die cavity. The surface of the *VD* area of the die cavity after 300 produced clinched joints showed only minor traces of wear for all three PVD coatings evaluated. Small spherical particles (Fig. 3) were removed by the material flow or even plastically deformed due to high levels of the contact pressure. This phenomenon was shown in Fig. 7 in CrN coating.

Conclusions. Three types of PVD coatings CrN, TiCN MP and ZrN were deposited on the surface of rigid dies for round mechanical clinching and experimentally tested by joining of two H220PD+Z steel sheets. Surfaces of individual die cavities were scanned by the scanning electron microscopy before mechanical joining. Individual die cavity was divided into specific areas: *OD*, *ROD*, *OVD*, *RVD*, and *VD*. SEM images showed no distinctive cases of wear or damage of all coatings that could negatively influence the proper function of the tool. Some areas, especially *OD* and *VD*, were covered with the small spherical particles that were present on the surface of die cavity, as well as coating surface due to LARC deposition process utilized. These particles were visible only when surfaces were scanned with higher magnifications. The EDX qualitative analyses confirmed chromium, titanium, and zirconium as the dominant elements for CrN, TiCN MP and ZrN coatings, respectively. The total number of 300 mechanically clinched joints were produced by each pair of tools (punch and die) and by each coating deposited. The samples with 900 mechanically clinched joints were prepared. Surfaces of die cavities were scanned by SEM again. Some galling was detected in the *RVD* area of die cavity covered with the CrN and ZrN coatings. This area remained intact in the case of TiCN MP coating. The EDX qualitative analysis confirmed the presence of zinc and iron in the *RVD* area of CrN and ZrN coatings. Relatively planar *VD* and *OD* areas were worn only slightly. Small spherical particles were removed from the surface by the material flow, or they were plastically deformed by the action of the normal and contact stresses. Compressive forces or stresses are the main driving factor for galling and adhesion. Levels of normal stress (in the *Y* direction) and material flow along with the location of the contact pressure maximum were evaluated by the FEA calculations. Tools (die and punch) were modeled as deformable solid bodies without coating. High levels of normal stress were evaluated in the areas where the galling wear was observed, which was *ROD* especially. Another highly loaded areas were *RVD* and *VD*. Maximum levels of contact pressure were detected in the areas *VD*, *RVD*, and *ROD.* The material flow at each stage of mechanical clinching, such as drawing, compression, and interlocking, showed the direction of material flows and loading curvature of the die cavity. Future work is envisaged on the evaluation of further changes of the worn area through surface microgeometry parameters, which could more precisely describe the elementary phenomena taking place.

Acknowledgments. This work was conducted under the research projects KEGA 065TUKE-4/2017 and VEGA 1/0441/17.

Р е з ю м е

Досліджується знос робочої частини механічного преса в процесі клінч-з'єднання листів із легованої високоміцної сталі H220PD+Z із гальванічним покриттям методом холодного формування (пуклівка). Точкове з'єднання листів здійснюється за допомогою жорсткого штампа та пуансона круглого перерізу малого діаметра (без рухомих частин) з інструментальної сталі з нанесеними PVD покриттями трьох типів: ZrN, CrN та TiCN MP. Знос робочої частини штампа з відповідним покриттям оцінюється після проведення 300 операцій пуклівки. Порівняння отриманих експериментальних даних із результатами скінченноелементного розрахунку свідчить про їх задовільну відповідність і підтверджує, що знос робочої частини штампа відбувається в основному поблизу кругової межі штампа та пуансона.

1. A. Breda, S. Coppieters, and D. Debruyne, "Equivalent modeling strategy for a clinched joint using simple calibration method," *Thin Wall. Struct.*, **113**, 1–12 (2017).
2. M. Eshtayeh, M. Hrairi, and A. K. M. Mohiuddin, "Clinching process for joining dissimilar materials: state of the art," *Int. J. Adv. Manuf. Tech.*, **82**, 179–195 (2016).
3. J. Mucha, "The analysis of lock forming mechanism in the clinching joint," *Mater. Design*, **32**, 4943–4954 (2011).
4. F. Lambiase and A. Di Ilio, "Finite element analysis of material flow in mechanical clinching with extensible dies," *J. Mater. Eng. Perform.*, **22**, 1629–1636 (2013).
5. K. Mori, N. Bay, L. Fratini, et al., "Joining by plastic deformation," *CIRP Ann. - Manuf. Techn.*, **62**, 673–694 (2013).
6. T. Gerstmann and B. Awiszus, "Recent development in flat-clinching," *Comp. Mater. Sci.*, **81**, 39–44 (2014).
7. S. Härtel, M. Graf, T. Gerstmann, and B. Awiszus, "Heat generation during mechanical joining processes – by the example of flat-clinching," *Procedia Engineer.*, **184**, 251–265 (2017).
8. Y. Zhang, H. Shan, Y. Li, et al., "Joining aluminum alloy 5052 via novel hybrid resistance spot clinching process," *Mater. Design*, **118**, 36–43 (2017).
9. Y. Futamura and M. Miura, "Characteristics of 780 MPa and 980 MPa grade hot-dip galvannealed steel sheets," *Kobelco Technol. Rev.*, No. 28, 3–7 (2008).
10. Y. Abe, S. Nihsino, K. Mori, and T. Saito, "Improvement of joinability in mechanical clinching of ultra-high strength steel sheets using counter pressure with ring rubber," *Procedia Engineer.*, **81**, 2056–2061 (2014).
11. J. P. Varis, "The suitability of round clinching tools for high strength structural steel," *Thin Wall. Struct.*, **40**, 225–238 (2002).
12. Y. Abe, T. Kato, and K. Mori, "Mechanical clinching of ultra-high strength steel sheets," in: Proc. of 14th Int. Conf. on Metal Forming (Sept. 16–19, 2012, Krakow, Poland), Wiley-VCH Verlag GmbH&Co KGaA, Weinheim (2012), pp. 615–618.
13. J. Varis, "Ensuring the integrity in clinching process," *J. Mater. Process. Tech.*, **174**, 277–285 (2006).
14. S. Zhang, *Thin Films and Coatings – Toughening and Toughness Characterization*, CRC Press, Taylor & Francis Group, New York (2016).
15. M. Wieland and M. Merklein, "Wear behavior of uncoated and coated tools under complex loading conditions," *Tribology in Industry*, **34**, 11–17 (2012).
16. J. Varis, "Economics of clinched joint compared to riveted joint and example of applying calculations to a volume product," *J. Mater. Process. Tech.*, **172**, 130–138 (2006).
17. O. Hahn, L. Budde, "Analyse und systematische einteilung umformtechnischer fugeverfahren ohne hilfsfugeteil," *Blech Rohre Profile*, **37**, 29–32 (1990).
18. J. Mucha, L. Kaščák, and E. Spišák, "The experimental analysis of forming an strength of clinch riveting sheet metal joint made of different materials," *Adv. Mech. Eng.*, **1**, 1–11 (2013).
19. D. A. Skobir, "High-strength low-alloy steels," *Mater. Technol*., **45**, 295–301 (2011).
20. J. Slota, *Computational Modeling of Sheet Metal Pressure* [in Slovak], Technical University of Košice, Košice, Slovakia (2017).

Received 25. 08. 2017